

Jun Wang
e-mail: davis.wjun@gmail.com

Zhigang Wang
e-mail: zgwang@ucdavis.edu

Weidong Zhu
e-mail: wdzhu@ucdavis.edu

Department of Mechanical and Aeronautical
Engineering,
University of California,
Davis, CA 95616

Yingfeng Ji
Department of Mechanical Engineering,
University of Wisconsin,
Milwaukee, WI 53211
e-mail: yfj@uwm.edu

Recognition of Freeform Surface Machining Features

This paper describes a method of machining feature recognition from a freeform surface based on the relationship between unique machining patches and critical points on a component's surface. The method uses Morse theory to extract critical surface points by defining a scalar function on the freeform surface. Features are defined by region growing between the critical points using a tool path generation algorithm. Several examples demonstrate the efficiency of this approach. The recognized machining features can be directly utilized in a variety of downstream computer aided design/computer aided manufacturing (CAM) applications, such as the automated machining process planning.
[DOI: 10.1115/1.3527075]

Keywords: machining feature recognition, freeform surface, Morse theory, region growing

1 Introduction

With the development of geometric modeling techniques, more and more complicated freeform surfaces can now be mathematically represented and designed for industrial products, including die/mold parts and aircraft parts with general computer aided design (CAD) systems. From the machining point of view, a freeform surface usually consists of more than one unique machining patch that can be machined with a single machining process. If these unique machining patches cannot be recognized before machining, it is difficult if not impossible to produce high-quality surfaces. Figure 1(a) shows a typical freeform surface, represented by a nonuniform rational B-spline (NURBS) surface. This freeform surface comprises two unique machining patches from the machining perspective. If the machining process plan, such as the tool path generation, is made for the entire surface instead of the two machining patches separately, jaggy and bumpy machining residuals will be generated on the surface after machining. Figure 1(b) shows the isoplanar tool path for the whole freeform surface, with which the pick feed and the scallop height are variable, and consequently the bumpy residual area will exist on the surface. Figure 1(c) shows the tool path based on the constant scallop height for the whole freeform surface. It can be observed that some of the tool paths cannot keep G1 continuity, which will inevitably damage the machining surface quality. Figure 1(d) gives surface recognition results with two unique machining patches. Based on the recognized patches, the tool path can then be generated to obtain a high-quality surface. Therefore, prior to machining, it is significantly imperative to recognize the unique machining patches of the freeform surface, specifically to segment the freeform surface into unique machining patches, to achieve the high-quality machining for the freeform surface.

In the past few years, a number of researchers have designed various algorithms to recognize and segment freeform surface models into features by using such methods as region growing [1,2], watershed [3], hierarchical clustering [4,5], skeleton [6], Reeb graph [7,8], and spectral analysis techniques [9] in CAD/computer aided manufacturing (CAM) and computer graphics [10].

Besl and Jain [1] took advantage of the region growing technique to segment a large image into regions of arbitrary shapes. They first implemented an initial segmentation by labeling the data points using the mean and Gaussian curvatures, which is then refined by an iterative region growing method based on the variable-order surface fitting. The algorithm is, however, sensitive to data noise and selection of thresholds. Mangan and Whitaker [3] extended the watershed technique from image processing to 3D mesh segmentation. They proposed a partition approach of 3D surface segmentation by defining the curvature as a watershed function, in which the surface was partitioned into patches such that each patch was bounded by areas of higher or different curvatures. With this method, some segment boundaries are jaggy and the oversegmentation problem occurs occasionally. Attene et al. [4] utilized the hierarchical clustering technique to segment triangle meshes into faces on which points could be best approximated by plane, sphere, or cylinder primitives. In this method, the user was able to interactively select the number of regions. The limitation of this method is that the number of surface primitives is relatively limited due to the manual selection by the user. Várady et al. [11] presented an algorithm for the segmentation of 3D models by the combinatorial Morse theory [12], in which they analyzed functions defined over manifolds. By using the hierarchical Morse complex technique, the coarse segmentation was initially obtained, and then the segmentation was refined using the skeleton construction and the computation of region boundaries. Natarajan et al. [13] described an inspiring method for segmenting a molecular surface with the Morse–Smale complex theory.

Sunil and Pande [14] devised an automatic algorithm to recognize features from freeform surfaces in sheet metal parts. The taxonomy of features in sheet metal parts was first given, and then the corresponding recognition criteria were defined. The region- and edge-growing-based segmentation method was adopted to decompose a model into meaningful regions. In the method, the critical region edge detection algorithm is based on triangular shape attributes, such as the needle triangle and the cap triangle, completely depending on the original input mesh. Lim et al. [15] designed an identification method for depression and protrusion (DP) features on freeform solids, in which the boundary edges of DP features were extracted with a partitioning algorithm and then the surface patches were easily generated to cover the depressions or to isolate the protrusions. It is effective for the model with apparent concave edges. However, this method cannot handle the

Contributed by the Computational Aided Manufacturing Committee of ASME for publication in the JOURNAL OF COMPUTING AND INFORMATION SCIENCE IN ENGINEERING. Manuscript received April 29, 2009; final manuscript received June 28, 2010; published online December 17, 2010. Assoc. Editor: S. Gupta.

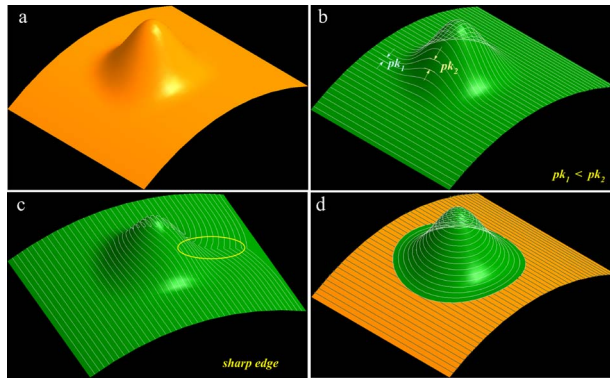


Fig. 1 Freeform surface recognition: (a) freeform surface, (b) isoplanar tool path generation without recognition, (c) isoscallop height tool path generation without recognition, and (d) tool path generation after recognition

identification of DP features, which are not bounded by edges in the 3D model. Sridharan and Shah [16,17] designed and implemented a comprehensive methodology for the recognition of multi-axis milling features, which was topological entity free, i.e., independent of the number of topological entities in a part. They first gave numerical control (NC) milling feature taxonomy, including cut-through, cut-around, and cut-on features. By analysis of the geometric characteristics and milling properties of each milling feature, the corresponding recognition criteria were presented accordingly.

From all the approaches briefly mentioned above, the same basic ideas behind feature recognition are (1) defining the features according to the specific applications and (2) formulating the corresponding recognition criteria of features. The definition of features is dependent on applications in two types: geometric based and machining based. For the first definition, the geometrical and topological characteristics of features are considered. Vergeest and co-workers [18,19] gave a general geometric formalism for freeform features. For the machining-based definition, besides the geometrical and topological properties, the machining information is also incorporated. Sridharan and Shah [16] presented a comprehensive definition for regular machining features. For our application, the machining features need to be recognized from general freeform surfaces. The recognition methods based on the geometric definition are not sufficient in our cases without considering the machining information. On the other hand, those recognition approaches with the machining definition can only deal with the regular machining features, such as pockets, slots, and holes, while they cannot cope with the recognition of general freeform, machining features. Therefore, we shall first give the definition of the freeform, machining feature and then present a novel algorithm to recognize these features. The freeform, machining feature is generally defined as the topologically adjacent surface patches that can be machined with a single machining process. With this definition, we shall construct the related recognition criteria using both geometric and machining characteristics of freeform surfaces.

2 Algorithm Overview

According to the machining theory [20], besides the tool path pattern, the vertical motion of a cutting tool during machining also has a significant influence on the machining surface quality. An unstable vertical motion makes the cutting tool undergo an uneven force, and the vibration of the cutting tool occurs on the machining area so that the jaggy machining residual will be generated. Therefore, to improve the machining quality, it is necessary to keep the vertical motion of the cutting tool stable and smooth on the machining area. Geometrically, the area from one extreme

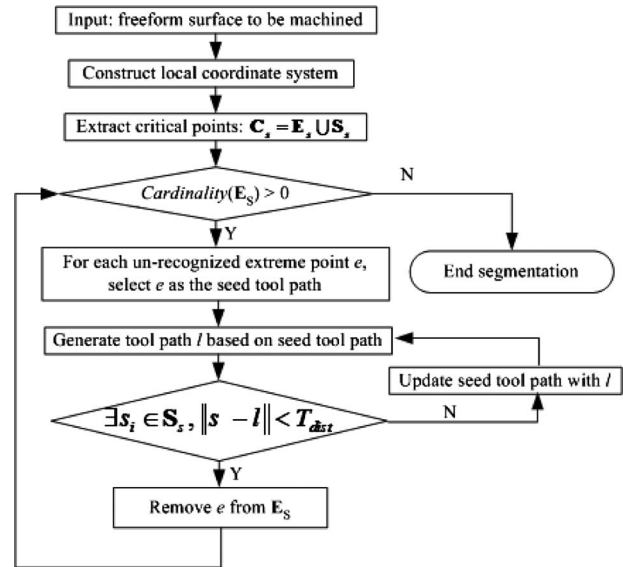


Fig. 2 Flowchart of segmentation algorithm

point to its closest saddle point possesses uniform geometric properties on the freeform surface [12]. For instance, the curvatures and slopes on the area vary continuously and smoothly, which directly determine the vertical motion of the cutting tool. Therefore, it is reasonable to machine all these areas from an extreme point to its closest saddle point on the freeform surface together with a single machining process. From the machining point of view, we consider the machining area, which can be machined with the same machining process as a unique machining patch—a machining feature. This can be geometrically converted into recognizing the topologically adjacent patch, which starts from an extreme point and ends at its closest saddle point, as a machining feature. Based on that, we design the machining feature recognition algorithm as in Fig. 2, where C_s , E_s , and S_s are the critical, extreme, and saddle point sets, respectively, and T_{ud} and T_{dist} are prespecified thresholds.

3 Surface Segmentation Algorithm

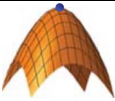
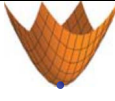
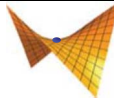

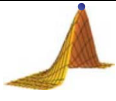
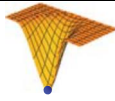
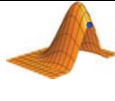
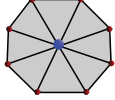
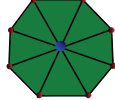
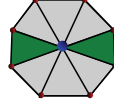
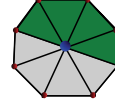
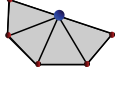
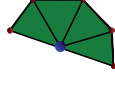
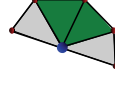
3.1 LCS Construction. Prior to NC machining, the workpiece orientation is a significantly important task, whose goal is to seek such an optimal orientation that the maximum number of faces of the workpiece could be machined in a single setup by using a flat-end or ball-end cutting tool. From the geometric perspective, the optimal objective of workpiece orientation can be translated into maintaining the sum of deviation in an angle minimal between the axis of the cutting tool and the normal vectors of all the points on the workpiece. This kind of problem was studied by Radzevich and Goodman [21] and Tang et al. [22] on the basis of an analysis of the Gaussian maps of workpiece and the cutting tool surface. The workpiece orientation method [21] is borrowed here to construct the local coordinate system (LCS) of the freeform surface in our algorithm. The main idea is to calculate the area-weighted mean normal of a given surface as the z-axis of the LCS of the surface.

Assume that the equation of the freeform surface S to be segmented is given as

$$S(u,v) = (x(u,v), y(u,v), z(u,v)) \quad (1)$$

where u and v are the parametric coordinates of a point on the surface S , and x , y , and z are the Cartesian coordinates of a point on S . The partial derivatives of S can be denoted by $S_u(u,v)$ and $S_v(u,v)$. Suppose the surface S consists of small patches, S_1, \dots, S_m , where i is the index of patches and m is the number of

Table 1 The link of critical points of two-manifold

Manifold without boundary				Manifold with boundary		
Maxima	Minima	Saddle	Regular	Maxima	Minima	Regular
						
						

patches of S . Let A_s and A_{s_i} be the area of surface S and the i th patch S_i , and then $A_s = \sum_{i=1}^m A_{s_i}$ and $A_{s_i} = \Delta u_i \times \Delta v_i$. Let C_i be the central point of patch S_i whose normal vector is parallel to the normal vector \mathbf{N}_{s_i} of the patch S_i . Then, the normal vector \mathbf{N}_s can be calculated by

$$\mathbf{N}_s = \mathbf{S}_u(u, v)|_i \times \mathbf{S}_v(u, v)|_i \quad (2)$$

For a discrete model of surface, the area-weighted average normal vector of the surface is described as

$$\mathbf{N}_s = \frac{\sum_{i=1}^m (\mathbf{N}_{s_i} \cdot A_{s_i})}{\sum_{i=1}^m (A_{s_i})} \quad (3)$$

The centroid CT_s of surface S is represented as

$$CT_s = \sum_{i=1}^m C_i \quad (4)$$

For the continuous model of the surface, the area-weighted average normal vector becomes

$$\mathbf{N}_s = \frac{\int_{A_s} \mathbf{n}(u, v) dA_s}{A_s} = \frac{\int \int_S \sqrt{E_s G_s - F_s^2} \cdot \mathbf{n}(u, v) du dv}{A_s} \quad (5)$$

where $\mathbf{n}(u, v)$ is the normal vector of point (u, v) on surface S , and E_s, G_s , and F_s are the coefficients of the first fundamental form of surface S (see Ref. [23] for details).

With the normal vector and the centroid of a surface, the LCS of the surface can be constructed. We consider the normal vector \mathbf{N}_s as the z -axis and the centroid CT_s as the origin. Then, a plane located at CT_s can be created with the normal \mathbf{N}_s . The bounding rectangle is obtained by projecting the freeform surface onto the plane. Finally, two orthogonal directions of the bounding rectangle are regarded as the x -axis and y -axis of the LCS. Once the LCS is constructed, the surface can be transformed from the LCS into the World Coordinate System (WCS) using the homogeneous transformation. The surface in the WCS can be computed by

$$\begin{bmatrix} S'(u, v) \\ 1 \end{bmatrix} = T \cdot \begin{bmatrix} S(u, v) \\ 1 \end{bmatrix} \quad (6)$$

where $S'(u, v)$ is the corresponding surface of $S(u, v)$ in the WCS and T is the general homogeneous transformation matrix.

3.2 Critical Point Extraction. The critical points of a freeform surface can be extracted by putting the surface into its LCS. To this end, we take advantage of the Morse theory [12]. In differential topology, the Morse theory gives a very direct way of analyzing the topology of a manifold by studying differentiable functions on that manifold. Morse originally applied his theory to geodesics and specifically studied the critical points of generic, smooth functions on manifolds.

Let M^2 be a closed two-manifold surface and $f: M^2 \rightarrow R$ a real valued smooth function. A point p is called the critical point of the function f if the gradient at this point vanishes ($\nabla f(p)=0$); other-

wise, it is regarded as a regular point. A critical point p of f is called nondegenerate if the Hessian matrix of f at p is nonsingular and is called degenerate otherwise. There are three kinds of nondegenerate critical points: minima, saddles, and maxima. The function f is called a Morse function if none of its critical points are degenerate. The local behavior of a Morse function at critical points can be represented by the Morse Lemma [24].

MORSE LEMMA. Let p_0 be a nondegenerate critical point of a smooth function $f: M^2 \rightarrow R$. Then, there exist local coordinates (X, Y) , with p_0 as the origin, in such a way that the function f can be expressed with respect to (X, Y) as

$$\begin{cases} f = X^2 + Y^2 + c \\ f = X^2 - Y^2 + c \\ f = -X^2 - Y^2 + c \end{cases} \quad (7)$$

where $c=f(p_0)$ and the number of the minus signals of f is called the index of p : $\text{index}(p)$, which can be utilized to classify critical points.

Case 1. For closed smooth manifolds, the index of a Morse critical point is equal to the number of negative eigenvalues of its Hessian matrix. A point v can be categorized in terms of the index number,

$$\begin{cases} (1) \text{ Minima: } \text{index}(v) = 0 \\ (2) \text{ Saddle: } \text{index}(v) = 1 \\ (3) \text{ Maxima: } \text{index}(v) = 2 \\ (4) \text{ Regular: } \text{index}(v) \neq 0, 1, 2 \end{cases} \quad (8)$$

Case 2. Since the freeform surface may be represented in a discrete way, such as by triangular meshes, we also introduce the extraction method for discrete manifolds. For closed discrete manifolds, Banchoff [25] originally extended the Morse theory to triangle meshes and showed that the extension is even more elementary than the smooth surface. In a two-manifold triangle mesh, the piecewise-linear function is defined on the vertices of the mesh, and its value is calculated by linear interpolation across the edges and the triangle patches of the mesh.

Here, we start with some definitions. The star $\text{star}(v)$ of a vertex v comprises all triangles incident to v and all vertices and edges of those triangles; the link $\text{link}(v)$ of v consists of all edges that are in the star of v and disjoint from v ; the lower link $\text{link}^-(v)$ of v is composed of the edges induced by vertices with a lower function value than that of v ; the higher link $\text{link}^+(v)$ of v consists of the edges induced by vertices with a higher function value than that of v ; the mixed link $\text{link}^\pm(v)$ of v consists of the edges induced by two vertices such that one vertex has a lower function value than v and the other has a higher function value than v . Then, a vertex can be classified into various critical points and regular points by means of the link properties of the vertex, as also shown in Table 1,

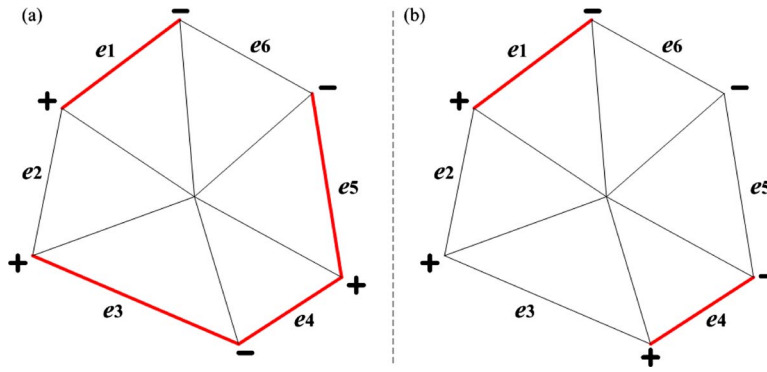


Fig. 3 The link of vertex

$$\begin{cases} (1) \text{ Minima: } \text{cardinality}(\mathbf{link}^-(v)) = 0 \\ (2) \text{ Saddle: } \text{cardinality}(\mathbf{link}^\pm(v)) = 2 + 2m (m > 0) \\ (3) \text{ Maxima: } \text{cardinality}(\mathbf{link}^+(v)) = 0 \\ (4) \text{ Regular: } \text{cardinality}(\mathbf{link}^\pm(v)) = 2 \end{cases} \quad (9)$$

where $\text{cardinality}(\mathbf{S})$ measures the number of elements in set \mathbf{S} and m means the multiplicity of the saddle point. Figure 3 gives an example. In Fig. 3(a), $\mathbf{link}^\pm(v) = \{e1, e3, e4, e5\}$ and its cardinality=4, so v is the saddle point; on the other hand, in Fig. 3(b), $\mathbf{link}^\pm(v) = \{e1, e4\}$ and its cardinality=2, so v is the regular point.

Case 3. The Morse theory can also be extended to manifolds with boundaries by considering them as a collection of submanifolds [26]. The extension theory is called the stratified Morse theory, in which the most dramatic restriction is that only the extreme point, i.e., no saddle point, of the Morse function is allowed to exist on boundaries of manifolds. Let M be the two-manifold surface with boundaries B_1, B_2, \dots, B_n , and then the surface M can be represented by $M = M_{in} \cup \cup_i B_i$, where M_{in} is the interior of M . The interior manifold M_{in} can be considered as the closed manifolds without boundaries, and hence its critical points can be handled by the foregoing criteria. For each boundary B_i , let p be an arbitrary point of B_i and $\mathbf{Nghbr}(p)$ be the vertex set of $\mathbf{star}(p)$, and then with the restriction of the stratified Morse theory in mind, we can determine the type of p with the criteria

$$\begin{cases} (1) \text{ Minima: } f(p) < f(q), \quad \forall q \in \mathbf{Nghbr}(p) \\ (2) \text{ Maxima: } f(p) > f(q), \quad \forall q \in \mathbf{Nghbr}(p) \\ (3) \text{ Regular: } \text{otherwise} \end{cases} \quad (10)$$

Table 1 gives the link of the critical points of the two-manifold. From the above criteria, we can see that critical points are always related to the Morse function, which is defined as a real valued function on a surface. There are various definitions of the Morse function in current applications. For instance, Hilaga et al. [27] defined a function whose value was given at each point by calculating the average geodesic distance to all points on the surface for the purpose of shape matching. Liu et al. [28] regarded a curvature function as the Morse function for extracting salient points from meshes. Since the workpiece orientation approach is used to orient the freeform surface in our method, many parts on the surface can be accessible from the orientation direction. Moreover, the orientation direction is selected as the z-axis of the LCS in Sec. 3.1. Therefore, it is basically appropriate to define the height function as the Morse function to extract critical points for freeform surfaces, especially for the 2.5D geometry. Figure 4 gives a comparison of critical point extraction with typical Morse functions. From the comparison, we note that the height function is more effective to be utilized as the Morse function to extract critical points of freeform surfaces in this instance. Particularly, there are some cases in which some parts in the surface cannot be

reachable even after orientation. Here, we take advantage of the mean curvature function as the Morse function to extract critical points.

3.3 Region Growing Process. After obtaining the critical points of the freeform surface, the region growing technique is exploited to recognize all included machining features. As mentioned above, one surface can be divided into unique machining patches, which could be machined by the same machining process parameters, including machine, cutting tool, tool path pattern, and so on. According to this machining characteristic, these machining process parameters are utilized in the region growing criterion to recognize machining features from the freeform surface. We grow all adjacent regions, which could be machined with the same tool path pattern by a cutting tool in a machine, and specifically grow the adjacent regions starting from an extreme point and terminating at its closest saddle point. The region growing process could be described as follows.

- (1) Select one extreme point of the surface as the seed (tool path) and initiate the region with the seed.
- (2) Generate the adjacent tool path of the seed on the unsegmented surface according to the appropriate tool path generation method and set it as the current tool path.
- (3) Calculate the shortest distance between the current tool path and saddle points of the surface.
 - (a) If the distance is larger than the predefined threshold,
 - (i) grow the region to the current tool path
 - (ii) update the seed as the current tool path and go to step (2)

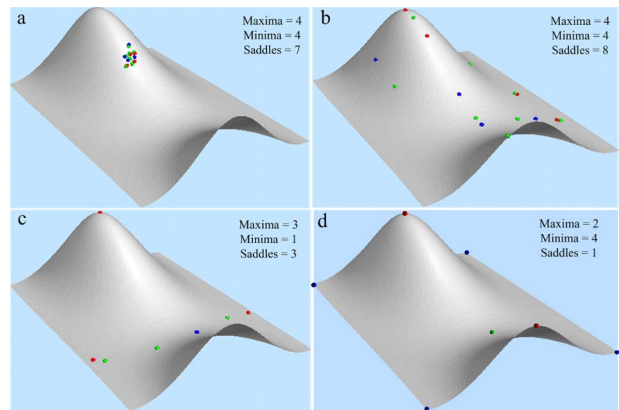


Fig. 4 Critical point extraction with different Morse functions: (a) mean curvature function, (b) least-squares projection function, (c) geodesic distance function, and (d) height function

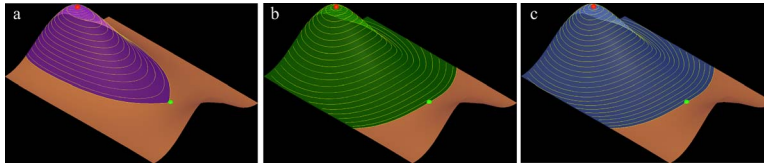


Fig. 5 Region growing with (a) isoplanar method, (b) iso-scallop height method, and (c) iso-pick feed method

- (b) Otherwise,
- (i) generate the adjacent tool path of the seed passing through the closest saddle point of the extreme point
 - (ii) grow the region to the adjacent tool path
 - (iii) terminate this region growing process and set the region as a unique machining patch—a machining feature

With the region growing process, the unique machining patches are automatically generated. Meanwhile, we note that sometimes there are a few parts on the surface that do not include critical points so that these parts remain unsegmented after finishing the region growing process. In this case, we regard each topologically disjoint unsegmented part as one unique machining patch. Then, the entire surface is completely decomposed into meaningful patches—machining features. Once all machining features have been recognized, we can apply the related tool paths to them for machining. Since the tool paths have already been generated for the features recognized by the region growing process, these existing tool paths can be used directly for machining. However, occasionally, there are such machining features that are not recognized by the region growing process that there are no existing tool paths for them. Moreover, as the adjacent machining features are joined at their common saddle points, it is necessary to blend the tool paths of these machining features at the saddle points and keep the joint machining area smooth. Thus, we would select other proper tool paths for these features, such as the boundary-conformed tool path generation [29].

For the region growing process, it is essentially based on the appropriate tool path generation scheme for the freeform surface. In our system, three kinds of typical region growing methods have been designed related to the corresponding tool path generation schemes.

- (1) *Isoplanar based region growing method.* In this method [30], tool paths are generated by intersecting a series of parallel planes with the surface, and the distance between two adjacent planes can be determined approximately by the scallop height requirement. The key point of this method is how to determine the orientation of parallel planes. Since we extract critical points of surface within the LCS, the z-axis of the LCS could be used to determine the orientation. Figure 4 shows this region growing result.
- (2) *Iso-scallop height based region growing method.* With the method [31,32], tool paths are evenly distributed across the surface so that the scallop height between two adjacent tool paths, a measure of surface quality, remains constant within a predefined tolerance. We assume that surface machining is operated with a ball-end cutting tool. Conceptually, the basic procedure of this method is given below.
 - (i) Offset the surface with the distance of the predefined tolerance regarding scallop height and get the scallop offset surface.
 - (ii) Offset the surface with the distance of radius of the cutting tool and get the tool center offset surface.
 - (iii) Select one tool path as the seed tool path.

- (iv) Sample the seed tool path into points and construct the Frenet frame at each sample point.
- (v) For each sample point, calculate the corresponding scallop peak point.
 - (a) Intersect the cutting tool envelope surface with the normal plane of the point and get the intersection curve.
 - (b) Intersect the curve with the scallop offset surface and get the scallop peak point.
- (vi) Fit all scallop peak points into the scallop curve.
- (vii) For each scallop peak point, determine the corresponding point on the next tool path.
 - (a) Construct the Frenet frame of the scallop curve at the scallop peak point.
 - (b) Create a circle in the normal plane of the Frenet frame with the scallop peak point as the center and the radius of the cutting tool as the radius.
 - (c) Intersect the circle with the tool center offset surface and get the tool center.
 - (d) Create a circle in the normal plane with the tool center as the center and the radius of the cutting tool as the radius, and then there must be an intersect point between the circle and the surface, which is referred to as the corresponding point of the scallop peak point.
- (viii) Fit all the corresponding points of the scallop peak points and get the next tool path of the seed tool path.
- (ix) Update the seed tool path as its next tool path and go to step (iv).

- (3) *Iso-pick feed based region growing method.* In this method, the tool path distributes on the surface with the same geodesic distance such that the maximal scallop height is limited in a prespecified tolerance. The main steps can be presented as follows.

- (i) Calculate the “safe” value of pick feed according to the maximal scallop height and the curvature of surface.
- (ii) Select one tool path as the seed tool path.
- (iii) Sample the seed tool path into points and construct the Frenet frame at each sample point.
- (iv) For each sample point, calculate the corresponding point on the next tool path.
 - (a) Intersect the normal of the Frenet frame with the surface and get an intersection curve.
 - (b) Find the corresponding point on the intersection curve with a geodesic distance of the safe value of pick feed to the sample point.
- (v) Fit all the corresponding points of the sample points and get the next tool path of the seed tool path.
- (vi) Update the seed tool path as its next tool path and go to step (iii).

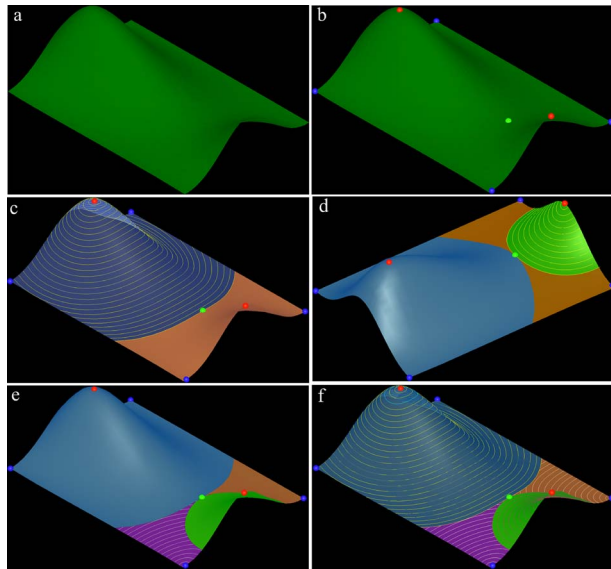


Fig. 6 Freeform surface recognition: (a) freeform surface, (b) critical point extraction, (c) region growing starting from a maximal point, (d) region growing from another maximal point, (e) region growing from a minimal point, and (f) recognized machining patches and their tool path

By using these three methods above, the region growing results of a freeform surface are given in Fig. 5. From the results, we can observe that the region growing methods based on the iso-scallop height and iso-pick feed are more effective than that based on isoplanar. Therefore, the latter two methods are more frequently utilized for a freeform surface.

4 Implementation Results and Discussion

The algorithm proposed has been implemented in our CAM system based on VISUAL C++ and OPENGL platforms. All kinds of freeform surfaces with IGES, STEP, or STL file format can be imported and processed in this system. A number of industrial models have been tested. Here, several typical examples are presented.

Figure 6(a) is a freeform surface of an industrial product. The critical points are extracted from the surface, which consist of two maximal points, four minimal points, and one saddle point (see Fig. 6(b)). From one of the maximal points, the seed point with a higher function value is selected to grow the region on the basis of

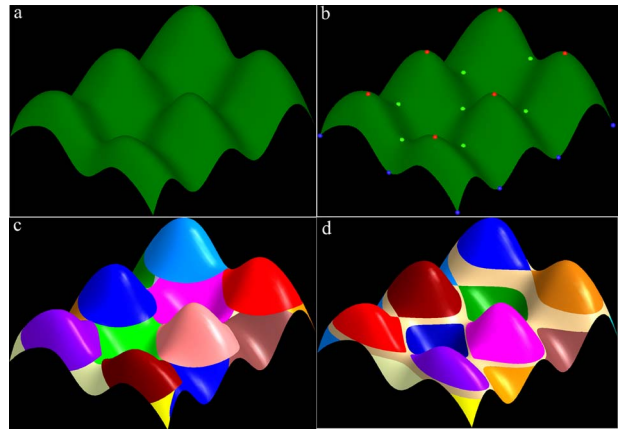


Fig. 7 Freeform surface recognition: (a) freeform surface, (b) critical point extraction, (c) iso-scallop height based segmentation, and (d) isoplanar based segmentation

the iso-pick feed method. Once the growing region reaches the saddle point, region growing will terminate, and hence one unique machining patch is obtained, which is labeled red in Fig. 6(c), while the green surface is unsegmented and needs to be further segmented. It should be noted that two minimal points are immersed and deleted by this region growing process (see Fig. 6(c)). After one region growing process finishes, one needs to check how many critical points are left on the unsegmented surface. For the remaining critical points on the unsegmented surface, similar steps are taken to get the final segmentation result. Figure 6(d) presents the region growing result from the second maximal point. Figure 6(e) gives the region growing result from a minimal point. Figure 6(f) shows segmented machining patches. In our instances, the order to select extreme points is based on the function value of these points. Basically, the maximal points are prior to the minimal points. Among the maximal or minimal points, the point with the bigger absolute function value has higher selection priority.

Figure 7(a) gives another complicated freeform surface. By the Morse theory, critical points can be extracted, as shown in Fig. 7(b), including six maximal points, ten minimal points, and seven saddle points. Using the region growing method based on the iso-scallop height, all machining patches can be recognized, as shown in Fig. 7(c). Figure 7(d) shows the recognition result by using the isoplanar based region growing method.

Figure 8 demonstrates the recognition and machining for a 3D

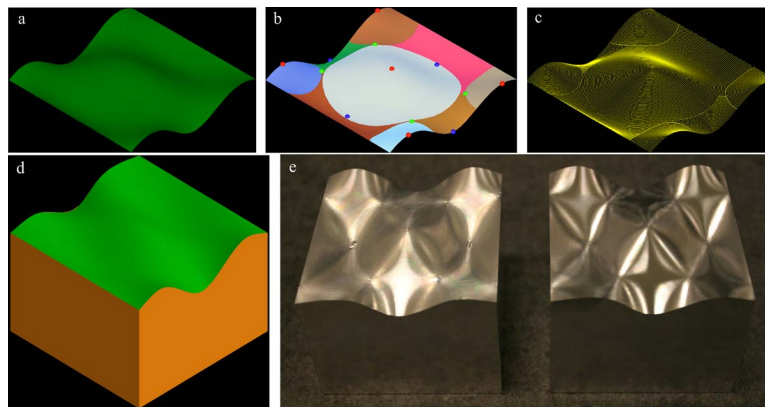


Fig. 8 Freeform surface recognition and machining: (a) freeform surface of 3D industrial model, (b) recognized machining patches, (c) iso-pick feed tool path generation, (d) CAD industrial model, and (e) surface machining comparison between ESPRIT Modular CAM processor and this proposed algorithm

industrial part ($65 \times 65 \times 40 \text{ mm}^3$). Figure 8(a) shows the freeform surface in the model. The critical points are extracted, and hence the nine machining features are recognized, as shown in Fig. 8(b), labeled with different colors. Based on the iso-pick feed tool path generation method, the corresponding tool path is generated for each machining feature, as shown in Fig. 8(c). Figure 8(d) is the original CAD model of the industrial part. Figure 8(e) shows the machined workpiece with the tool path generated by an ESPRIT[®] Mold CAM processor [33] and the proposed algorithm. During the machining, a 6 mm diameter ball-end milling cutter is used, and a maximum scallop height of $20 \mu\text{m}$ is set. The machining times are around 6.5 h and 4.2 h. Using the processor, the upper freeform surface is regarded as a single surface, instead of several machining features, so that a lot of noncutting time is wasted. Moreover, the freeform surface is machined indiscriminately with the processor so that there are some machining residual areas, especially located at the peak and pit of the surface, and the machined workpiece is bumpy and jaggy on the left side of Fig. 8(e). By comparison, the right-side workpiece, machined feature by feature with our method, is uniformly smooth.

5 Conclusions

In this paper, a novel method is proposed and implemented to recognize the freeform surface machining features from CAD models. We present three extraction criteria of critical points, which are applicable not only to closed manifolds, but also to open manifolds with boundaries. Three region growing approaches related to tool path generation methods are given to recognize machining features effectively. Meanwhile, the corresponding tool path for each segmented patch has been generated automatically. In this algorithm, the geometric properties, such as normal vector and critical point, are exploited, while the machining characteristics, including tool path pattern and vertical motion of cutting tools, are also utilized to recognize the unique machining patches, which fairly facilitate the automation of the effective machining process planning of freeform surfaces. Based on this algorithm, a prototype system is developed and tested with typical freeform surfaces from mechanical products, demonstrating the high quality of the machining surfaces produced by the proposed method.

Also, there are some interesting problems in our system to be solved in our future research. What is a proper segmentation when there is no saddle point? According to our current method, the entire surface will be considered as a single surface, which is probably not appropriate. Thus, further research is also needed to cope with this situation. In addition, our method assumes that all parts of surface to be machined are accessible with one workpiece orientation. If there are some parts that are not reachable in a single orientation, we can apply this proposed recognition method to those remaining parts for recognizing them. Here, the problem regarding how to smoothly blend the joint area of features recognized from different orientations remains to be investigated.

References

- [1] Besl, P. J., and Jain, R., 1988, "Segmentation Through Variable-Order Surface Fitting," *IEEE Trans. Pattern Anal. Mach. Intell.*, **10**(2), pp. 167–192.
- [2] Lavoué, G., Dupont, F., and Baskurt, A., 2004, "Curvature Tensor Based Triangle Mesh Segmentation With Boundary Rectification," *IEEE Computer Graphics International, Crete, Greece, P. Trahanias, and S. Orphanoudakis, eds.*, pp. 10–17.
- [3] Mangan, A. P., and Whitaker, R. T., 1999, "Partitioning 3D Surface Meshes Using Watershed Segmentation," *IEEE Trans. Vis. Comput. Graph.*, **5**(4), pp. 308–321.
- [4] Attene, M., Falcidieno, B., and Spagnuolo, M., 2006, "Hierarchical Mesh Segmentation Based on Fitting Primitives," *Vis. Comput.*, **22**(3), pp. 181–193.

- [5] Katz, S., and Tal, A., 2003, "Hierarchical Mesh Decomposition Using Fuzzy Clustering and Cuts," *ACM Trans. Graphics*, **22**(3), pp. 954–961.
- [6] Lien, J. M., Keyser, J., and Amato, N. M., 2006, "Simultaneous Shape Decomposition and Skeletonization," *Proceedings of the ACM Solid and Physical Modeling Symposium*, R. Martin, and S. Hu, eds., pp. 219–228.
- [7] Berretti, S., Bimbo, A. D., and Pala, P., 2006, "Partitioning of 3D Meshes Using Reeb Graphs," *Proceedings of the 18th International Conference on Pattern Recognition*, Y. Tang, P. Wang, G. Lorette, and D. Yeung, eds., New York, pp. 19–22.
- [8] Antini, G., Berretti, S., Bimbo, A. D., and Pala, P., 2005, "3D Mesh Partitioning for Retrieval by Parts Applications," *Proceedings of the IEEE International Conference on Multimedia and Expo, The Netherlands, A. Smeulders, J. Biemond, M. Kersten, and P. Werkhoven, eds.*, pp. 1210–1213.
- [9] Liu, R., and Zhang, H., 2004, "Segmentation of 3D Meshes Through Spectral Clustering," *Pacific Conference on Computer Graphics and Applications*, Seoul, Korea, D. Cohen-Or, H. Ko, D. Terzopoulos, and J. Warren, eds., pp. 298–305.
- [10] Agathos, A., Pratikakis, I., Perantonis, S., Sapidis, N., and Azariadis, P., 2007, "3D Mesh Segmentation Methodologies for CAD Applications," *Computer-Aided Design and Applications*, **4**(6), pp. 827–841.
- [11] Várady, T., Facello, M. A., and Terék, Z., 2007, "Automatic Extraction of Surface Structures in Digital Shape Reconstruction," *Comput.-Aided Des.*, **39**(5), pp. 379–388.
- [12] Milnor, J., 1963, *Morse Theory*, Princeton University Press, Princeton, NJ.
- [13] Natarajan, V., Wang, Y., Bremer, P. T., Pascucci, V., and Hamann, B., 2006, "Segmenting Molecular Surfaces," *Comput. Aided Geom. Des.*, **23**(6), pp. 495–509.
- [14] Sunil, V. B., and Pande, S. S., 2008, "Automatic Recognition of Features From Freeform Surface CAD Models," *Comput.-Aided Des.*, **40**(4), pp. 502–517.
- [15] Lim, T., Medellin, H., Torres-Sanchez, C., Corney, J. R., Ritchie, J. M., and Davies, J. B. C., 2005, "Edge-Based Identification of DP-Features on Free-Form Solids," *IEEE Trans. Pattern Anal. Mach. Intell.*, **27**(6), pp. 851–860.
- [16] Sridharan, N., and Shah, J., 2004, "Recognition of Multi Axis Milling Features: Part I—Topological and Geometric Characteristics," *ASME J. Comput. Inf. Sci. Eng.*, **4**(3), pp. 242–250.
- [17] Sridharan, N., and Shah, J. J., 2005, "Recognition of Multi-Axis Milling Features: Part II—Algorithms & Implementation," *ASME J. Comput. Inf. Sci. Eng.*, **5**(1), pp. 25–34.
- [18] Vergeest, J. S. M., Horváth, I., and Spanjaard, S., 2007, "Parameterization of Freeform Features," *Proceedings of the International Conference on Shape Modeling and Applications*, Genova, Italy, p. 20.
- [19] van den Berg, E., Bronsvoort, W. F., and Vergeest, J. S. M., 2002, "Freeform Feature Modelling: Concepts and Prospects," *Comput. Ind.*, **49**(2), pp. 217–233.
- [20] Boothroyd, G., and Knight, W. A., 2005, *Fundamentals of Machining and Machine Tools*, Taylor & Francis, London.
- [21] Radzevich, S. P., and Goodman, E. D., 2002, "Computation of Optimal Workpiece Orientation for Multi-Axis NC Machining of Sculptured Part Surfaces," *ASME J. Mech. Des.*, **124**(2), pp. 201–212.
- [22] Tang, K., Woo, T., and Gan, J., 1992, "Maximum Intersection of Spherical Polygons and Workpiece Orientation for 4- and 5-Axis Machining," *ASME J. Mech. Des.*, **114**(3), pp. 477–485.
- [23] do Carmo, M., 1976, *Differential Geometry of Curves and Surfaces*, Prentice-Hall, Englewood Cliffs, NJ.
- [24] Matsumoto, Y., 2002, *An Introduction to Morse Theory*, translated from Japanese by K. Hudson and M. Saito, American Mathematical Society, Providence.
- [25] Banchoff, T. F., 1970, "Critical Points and Curvature for Embedded Polyhedral Surfaces," *Am. Math. Monthly*, **77**(5), pp. 475–485.
- [26] Goresky, M., and MacPherson, R., 1988, *Stratified Morse Theory*, Springer-Verlag, Berlin.
- [27] Hilaga, M., Shinagawa, Y., Komura, T., and Kunii, T. L., 2001, "Topology Matching for Full Automatic Similarity Estimation of 3D Shapes," *Proceedings of SIGGRAPH*, Los Angeles, CA, L. Pocock, ed., pp. 203–212.
- [28] Liu, Y. S., Liu, M., Kihara, D., and Ramani, K., 2007, "Salient Critical Points for Meshes," *Proceedings of the 2007 ACM Symposium on Solid and Physical Modeling*, Beijing, China, S. Hu, H. Qin, B. Levy, and D. Manocha, eds., pp. 277–282.
- [29] Yang, D. C. H., Chuang, J. J., and Oulee, T. H., 2003, "Boundary-Conformed Toolpath Generation for Trimmed Free-Form Surfaces," *Comput.-Aided Des.*, **35**(2), pp. 127–139.
- [30] Huang, Y., and Oliver, H. J., 1992, "Non-Constant Parameter NC Tool Path Generation on Sculptured Surfaces," *Int. J. Adv. Manuf. Technol.*, **9**(5), pp. 281–290.
- [31] Feng, H., and Li, H., 2002, "Constant Scallop-Height Tool Path Generation for Three Axis Sculptured Surface Machining," *Comput.-Aided Des.*, **34**(9), pp. 647–654.
- [32] Suresh, K., and Yang, D. C. H., 1994, "Constant Scallop-Height Machining of Free-Form Surfaces," *ASME J. Eng. Ind.*, **116**, pp. 253–259.
- [33] <http://www.dptechnology.com/en/index.asp>